JMEPEG (2020) 29:5574–5581
https://doi.org/10.1007/s11665-020-04895-7

1059-9495/$19.00

Sinterability of Silicon Carbide and Boron Carbide under Single-Mode Microwave Fields

Selva Vennila Raju, Michael Kornecki, and Raymond E. Brennan

(Submitted November 7, 2019; in revised form May 19, 2020; published online June 19, 2020)

The feasibility of processing silicon carbide (SiC) and boron carbide (B_4C) using a 2.45 GHz single-mode microwave system has been investigated. In order to determine the appropriate sintering conditions, samples were processed under various electric/magnetic (*E*/*H*) field ratios. Proportional 50% *E*/*H*-field ratios and 100% *H*-field conditions resulted in higher sample temperatures up to 1500 °C under equivalent microwave power. Sinterability was improved by adding B_4C and carbon to SiC, but limited to a thin outer layer of the pellet. While partial densification was observed under all conditions, isolated regions of full densification in microwave-processed B_4C samples were observed under 100% *H*-field mode. Microstructural analysis of microwave-processed SiC with and without additives indicated non-uniform sintering, while B_4C showed evidence of relatively homogeneous microstructures.

Keywords carbides, microstructure, microwave processing, x-ray diffraction

1. Introduction

Ultrafast sintering techniques such as microwave and flash sintering have gained interest in ceramic industries for their potential to significantly reduce processing temperatures and times, while influencing microstructural control and phase behavior (Ref 1-3). Microwave processing has led to rapid sintering of ceramics, metals, and ceramic–metal composites at drastically reduced temperatures compared to conventional sintering techniques. Processing times have been reduced from hours to minutes, while sintering temperatures have been lowered by several hundreds of degrees, yielding dense materials with finer grain structures. By avoiding the extreme conditions typically required to process advanced ceramic materials, energy savings and cost reductions have also been realized (Ref 3-7). Microwave susceptors, or absorbers, have also been introduced to improve coupling with microwave fields and enhance the heating response of selected samples. Carbon, for example, has been utilized as an excellent microwave susceptor (Ref 8-10), as it has demonstrated improvement in sinterability.

Two ceramic systems that have been explored using microwave sintering include SiC and B_4C, which are critical for use in protective systems that require low density and high strength, hardness, and thermal shock resistance. Both materials have been widely considered as the hardest commercially available materials next to diamond and cubic boron nitride, but also suffer from densification issues and poor crack resistance. Processing of pure, 100% dense SiC and B_4C through conventional sintering methods has been difficult to achieve, as both are highly covalently bonded materials and require sintering temperatures of 2000 °C or higher (Ref 11, 12). In addition, sintering of SiC has often resulted in discontinuous grain growth (Ref 13-17), requiring pressure application during heat treatment and incorporation of sintering aids to improve processing. In order to address these concerns, researchers have found that the addition of 5 wt.% B_4C has promoted homogeneous grain growth in SiC (Ref 18, 19), while introduction of carbon has resulted in enhancement of mechanical properties for both SiC and B_4C (Ref 20, 21).

Many research studies on microwave sintering of carbides and borides have been carried out using multi-mode microwave sintering. Studies conducted on SiC have resulted in theoretical densities of 96.38% and hardness values as high as 24.88 GPa (Ref 22, 23). In addition, lower sintering temperatures and reduced processing times for B_4C-Al and SiC-Al ceramic composites have been reported, resulting in significant energy savings (Ref 23).

As an alternative to multi-mode microwave processing, single-mode microwave (SMMW) sintering has been used to separate electric and magnetic field components using a resonant cavity as the sample chamber. This technique has proven to be advantageous over multi-mode microwave configurations that simultaneously excite tens to hundreds of modes. SMMW systems have enabled greater thermal control by exposing samples to specified electric and magnetic field ratios at microwave frequencies. These parameters have been further exploited to optimize material responses by strategically selecting material constituents that target the desired field components (Ref 24). These unique field conditions have also shown significant differences in heating behavior, based on the nature of the dielectric and magnetic responses found in numerous metals and oxide ceramics, including tungsten carbide, when processed in a 2.45 GHz SMMW cavity (Ref 25-28). It was concluded that conductive metal powders and

This article is an invited paper selected from presentations at the "11th International Symposium on Green and Sustainable Technologies for Materials Manufacturing and Processing," held during Materials Science & Technology (MS&T'19), September 29–October 3, 2019, in Portland, OR, and has been expanded from the original presentation.

Selva Vennila Raju, Oak Ridge Associated Universities, Belcamp, MD; **Michael Kornecki**, SURVICE Engineering, Belcamp, MD; and **Raymond E. Brennan**, CCDC Army Research Laboratory, Aberdeen, MD. Contact e-mail: raymond.e.brennan.civ@mail.mil.

tungsten carbide heated effectively under magnetic field conditions, while pure ceramic samples (mostly insulating) displayed higher heating rates under pure electric fields.

In the present work, a systematic study on sinterability of pure un-doped monolithic SiC, monolithic B_4C, and SiC-B_4C composites with carbon addition have been studied using a 2.45 GHz SMMW system by comparing heating and sintering behaviors under various field conditions.

2. Experimental

A 2.45 GHz SMMW system with 2 kW of adjustable microwave energy (Fig. 1a) was utilized for heat treatment of samples. A Modline-5R dual-band two-color pyrometer from IRCON, Inc. (Everett, WA, USA), with an operating range of 700 °C to 1800 °C was used to monitor sample temperatures. The sample mounting assembly parts shown in Fig. 1(b) were fabricated out of a high-purity porous alumina (Al_2O_3) SALI board from ZIRCAR Ceramics (Florida, NY, USA).

Powders of SiC (UF-25) and B_4C (171-HCSt) from H.C. Starck (Euclid, OH, USA) were used for microwave sintering studies. A SiC-B_4C-C composition was also prepared by ball milling 85 wt.% SiC, 5 wt.% B_4C, 10 wt.% Carbon Black (Monarch 120) from Cabot Corp. (Billerica, MA, USA), and SiC milling media, in a Nalgene bottle for 72 h at 60 rpm. In order to prepare for microwave sintering, as-received SiC, B_4C, and ball-milled SiC-B_4C-C powders were pressed into pellets. The ~ 13-mm-diameter, ~ 4.5-mm-thick pellets were die pressed and cold isostatically pressed at 207 MPa to form green bodies. The resulting pellets were placed in the single-mode microwave chamber, with the iris and plunger nominally positioned at resonant *E*/*H*-field conditions. Microwave emission was initiated at a power level of 11%, as measured by the magnetron power supply. Cavity resonance was adjusted using the variable short/iris configuration and verified by measuring the reflected power in the system. During each experimental run, the power was gradually increased by 1% increments while continuously tuning the waveguide until the sample reached a maximum steady-state temperature. Heating rates of approximately 10 °C/s were achieved. Samples were held for 30 min at these maximum temperatures, after which the microwave generator was shut off to allow them to cool rapidly. However, plasma formation and decoupling often inhibited the ability to hold at steady temperatures for extended periods. During plasma events, drastic reductions in temperature occurred. The characteristic impedance of the cavity changed due to the presence of the plasma, and the sample cavity required re-tuning in order to eliminate it and re-establish the maximum temperature. A second pellet made out of the sample material was used as a support disk in order to avoid any possible contamination from the porous Al_2O_3 sample mount. Table 1 shows the experimental conditions of various specimens sintered using SMMW under a flowing nitrogen atmosphere. A separate unprocessed pellet was used for each experimental run.

Temperature was measured in increments of microwave power under various *E*/*H*-field conditions as a function of time and power for SiC, B_4C, and SiC-B_4C-C, as shown in Fig. 2 and 3. It can be noted that the sample reached its highest temperatures under 50% *E*/*H*-fields and 100% *H*-field conditions. For the SiC and SiC-B_4C-C specimens, a temperature difference of 350 °C was observed between the 100% *H*-field and 100% *E*-field conditions at the same microwave power, while a difference of 500 °C was observed for B_4C. A similar response was observed for both SiC and B_4C specimens under various *E*/*H*-field conditions, as noted in Fig. 2 and 3. The behavior of SiC, B_4C, and SiC-B_4C-C systems was in direct contrast to typical ceramics observed under microwave fields, as oxide ceramics have been reported to demonstrate high microwave absorption under *E*-field compared to *H*-field conditions (Ref 26). This result suggested that SiC-B_4C-C and B_4C samples had higher magnetic losses than dielectric or conductive losses. Heating rates were a few hundred degrees per minute, with the highest rates achieved under the 100% *H*-field condition for both systems.

Particle size distribution analysis was performed using a PARTICA LA-960 Horiba Scientific (Piscataway, NJ, USA), and surface area measurements were carried out on the raw powders using a Micrometrics TriStar II Plus unit (Norcross, GA, USA) based on the multilayer physisorption of gas method

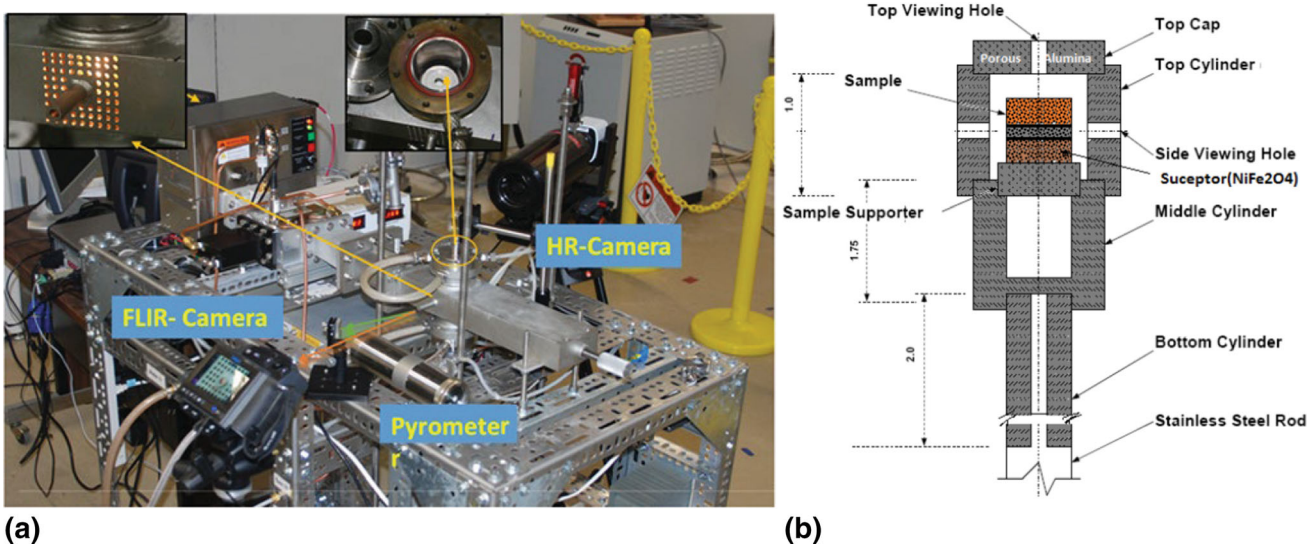

Fig. 1 (a) Experimental setup of 2.45 GHz single-mode microwave system, (b) sample mount assembly

Table 1 Experimental conditions of SMMW samples. All experiments were carried out under N_2 atmosphere and held at the maximum temperatures for 30 min

Expt. #	Sample	Height, mm	Susceptor	%*E*	%*H*	T_{max}, C
Run-1	SiC	2.23	None	0	100	1450
Run-2	SiC-B_4C-C	4.65	Sample	100	0	1100
Run-3	SiC-B_4C-C	2.20	Sample	50	50	1450
Run-4	SiC-B_4C-C	4.42	Sample	0	100	1450
Run-5	B_4C	4.63	Sample	100	0	1050
Run-6	B_4C	4.65	Sample	50	50	1400
Run-7	B_4C	4.67	Sample	0	100	1500

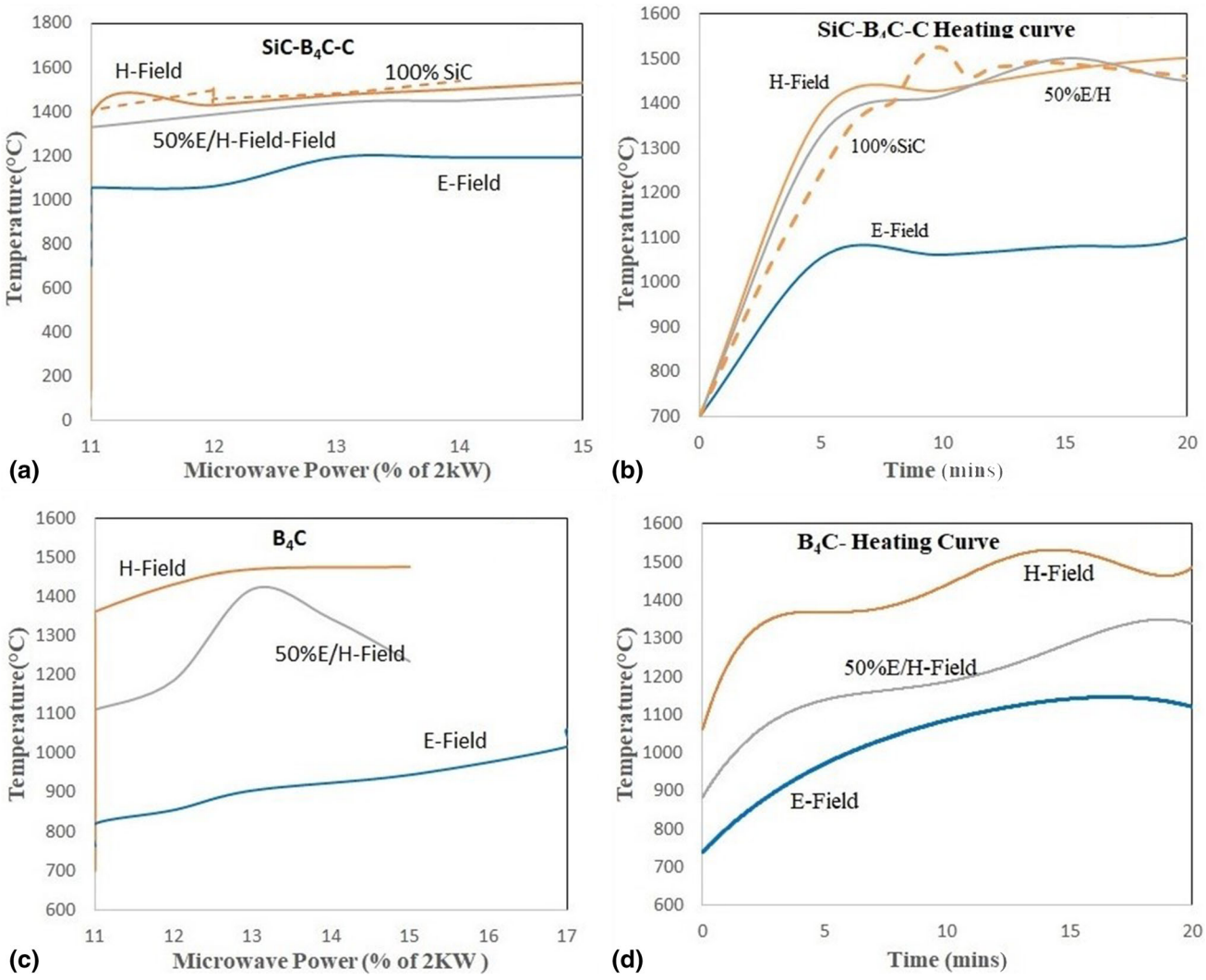

Fig. 2 Power, temperature, and time dependence of samples under various *E*/*H* microwave field conditions, including (a) temperature vs. power curve of SiC-B_4C-C (b) temperature vs. time curve of SiC-B_4C-C (c) temperature vs. power curve of B_4C, and (d) temperature vs. time curve of B_4C. Dashed lines represent SiC without any additives

by Brunauer, Emmett, and Teller (BET) (Ref 29), according to International Union of Pure and Applied Chemistry (IUPAC) recommendations from 1984 (Ref 30) and 1994 (Ref 31), as shown in Table 2.

X-ray diffraction (XRD) data were collected using a Bruker AXS D8 Phaser with a scintillation detector (Madison, WI, USA) at a Cu K-alpha wavelength of 1.5406 Å from 20° to 80° (two angles). XRD data of the microwave-sintered samples are shown in Fig. 3. XRD patterns collected from the microwave-processed samples confirmed that no phase changes occurred under microwave fields.

Microwave-sintered SiC, B_4C, and SiC-B_4C-C pellets were cross sectioned and mechanically polished down to 0.1 microns for scanning electron microscopy (SEM). Microstructural

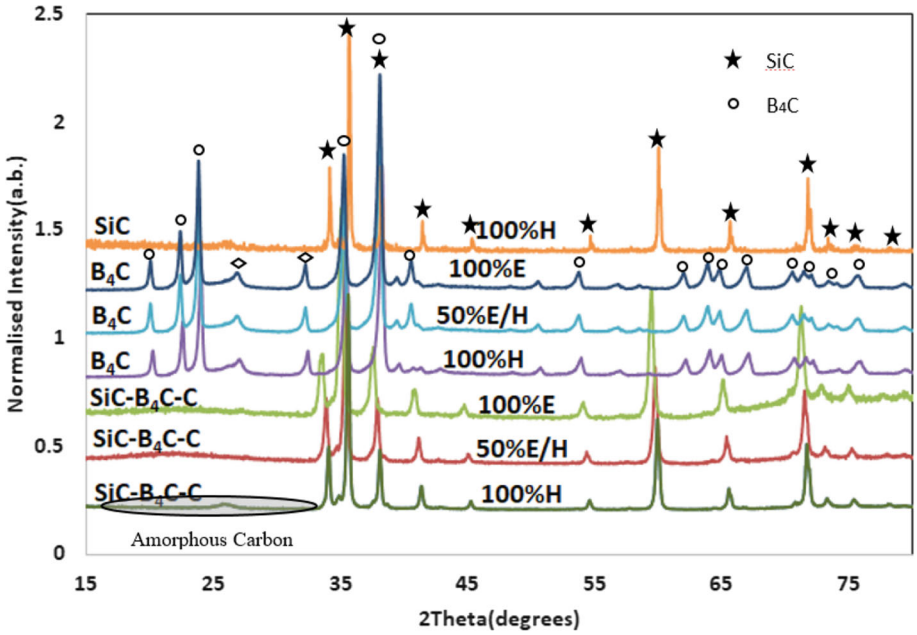

Fig. 3 X-ray diffraction data collected after sintering at Cu K-alpha wavelength of 1.56 Å under various *E*/*H* microwave field conditions

Table 2 Particle size distribution and surface area measurements of SiC and B_4C powders

Powder in dry mode	Median	Avg ± SD, μm	Covariance	Surface area, m^2/g
B_4C	D10	0.397 ± 0.004	1.0	15.078 ± 0.018
(HC Starck, Lot #1711/02)	D50	1.595 ± 0.059	3.7	
	D90	3.919 ± 0.095	2.4	
SiC	D10	0.080 ± 0.010	1.7	21.684 ± 0.087
(UF25), HC Starck Lot #4114)	D50	0.930 ± 0.010	2.3	
	D90	1.380 ± 0.024	1.0	

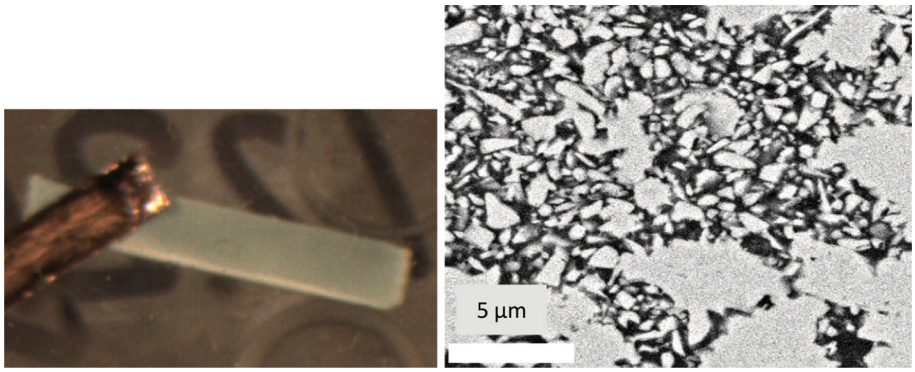

Fig. 4 SEM image of SiC microwave-sintered under 100% *H*-field at 1450 °C and held for 30 min, representing polished cross sections. Images show larger grains at the edges compared to the center

images, which were captured in backscattering mode, are shown in Fig. 4-9.

3. Results and Discussion

SiC pellets sintered under microwave fields were analyzed using optical microscopy and SEM, with microstructures shown in Fig. 4. Sintered regions were observed along the bottom edge of the sample, which was in contact with Al_2O_3. This was likely due to Al diffusion from the porous Al_2O_3 base at elevated temperatures. Energy-dispersive x-ray spectroscopy (EDS) analysis of the polished and cross-sectioned surfaces confirmed the presence of SiC, in addition to several Al_2O_3 particles. Agglomerated silica particles were also present on the interface between the upper surface, which exhibited a lower temperature, and the center region, which exhibited a higher temperature.

SEM images of SiC-B_4C-C showed regional evidence of sintering under 50% *E*/*H*-fields and 100% *H*-fields, while temperatures were significantly lower under 100% *E*-fields. SEM images of SiC and B_4C samples revealed white nanoscale particles on the larger grains at the surface of the pellet, indicating oxide formation.

SiC and B_4C phases remained unaltered, though smaller peaks of B_2O_3 were observed for samples sintered under 50% *E*/*H*-field and 100% *H*-field conditions. The resulting percentages of theoretical density and measured density are listed in Table 3. Archimedes measurements revealed low sample densities in the range of 1.6 to 1.8 g/cm^3, which indicated partial densification.

Samples processed under 50% *E*/*H*-field and 100% *H*-field conditions resulted in pore formation along the outer edges. EDS analysis confirmed the presence of B_4C and SiC particles, in addition to oxide formation along the unpolished surfaces. Figure 5 through 7 shows optical images of the cross-sectioned and polished specimens and their respective microstructures.

Table 3 Densities of microwave-sintered samples measured using Archimedes method, and corresponding theoretical density values

Run#	Sample name	%*E*	%*H*	ρ, g/cm^3	%TD
1	SiC	0	100	1.73	53.8
2	85%SiC-5%B_4C-10%C	100	0	1.84	57.3
3	85%SiC-5%B_4C-10%C	50	50	1.89	59.0
4	85%SiC-5%B_4C-10%C	0	100	1.86	58.0
5	B_4C	0	100	1.60	63.4
6	B_4C	50	50	1.62	64.2
7	B_4C	100	0	1.63	64.6

Figure 5 and 6 shows evidence that temperatures at the sample edges were higher than at the sample centers, which coincided with the carbon-rich regions along the outer edges, as confirmed by EDS. The quasi-metallic nature of the samples, which is likely due to the addition of carbon and the change in conductivity with temperature, may have limited the microwave power to regions along the outer surface. This skin effect is typically observed in metal samples after microwave sintering (Ref 32). Pellets were held at maximum temperatures for 30 min before shutting off the microwave power in order to enable rapid cool down of the specimens.

B_4C pellets were sintered under 100% *E*-field, 50% *E*/*H*-field, and 100% *H*-field microwave conditions, reaching maximum temperatures of 1050, 1300, and 1500 °C, respectively, as measured using the Modline-5R two-color pyrometer. During each experiment, the pellets were held at the maximum temperature for 30 min before rapidly cooling down to room temperature. Microstructures of B_4C sintered under various microwave field ratios appeared to be similar. However, the 100% *H*-field sample showed regions of fully dense B_4C (Fig. 8). Optical images of the B_4C pellets in Fig. 7 suggest that the temperature at the center of the sample could have been several hundred degrees higher than the surface temperature measured using the pyrometer. Fully dense B_4C regions were identified at the center of the specimen. In addition, several areas containing cracks were observed near the fully dense regions, likely due to thermal gradients from local hot spots that caused thermal expansion mismatch between fully and partially dense regions during microwave processing.

Ceramic materials, in general, are insulating and weakly conductive, with high dielectric losses, though ceramic insulators such as Al_2O_3 and ZrO_2 couple effectively under *E*-fields (Ref 22). On the other hand, carbides have demonstrated both conducting (i.e., WC, SiC) and non-conducting (i.e., B_4C)

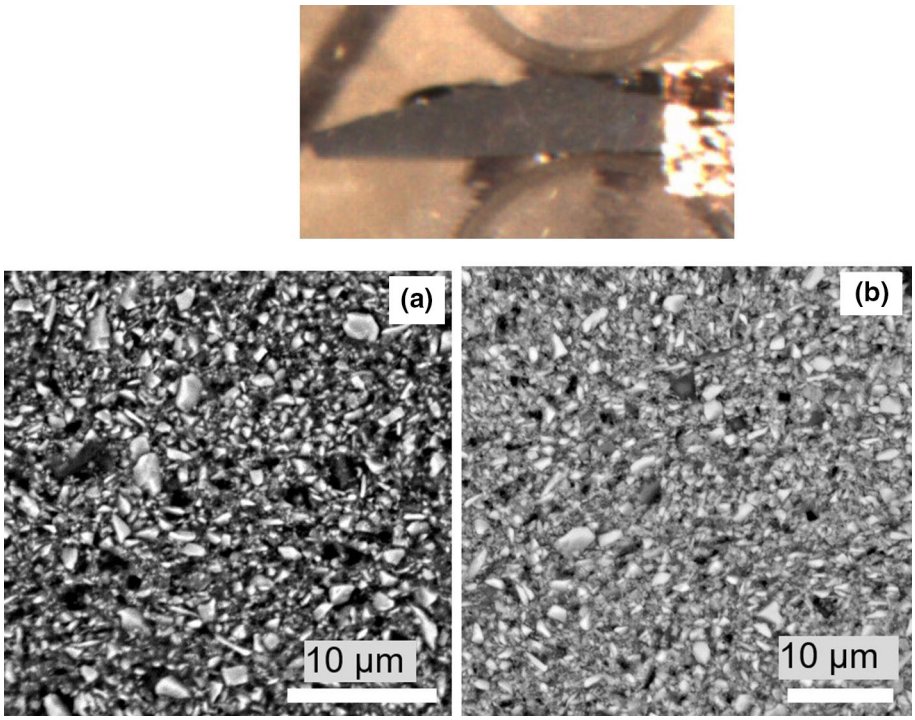

Fig. 5 SEM images of SiC-B_4C-C sintered under 100% *E*-fields and held at 1100 °C for 30 min, representing the (a) center and (b) edge of the polished cross-sectional region

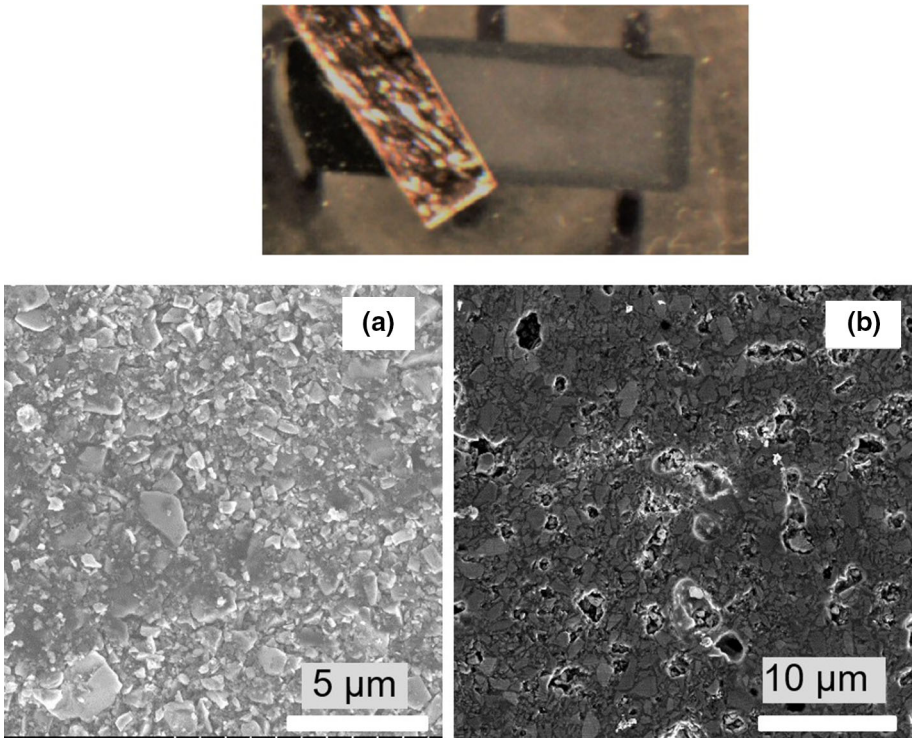

Fig. 6 SEM images of SiC-B_4C-C sintered under 50% *E*/*H*-fields and held at 1450 °C for 30 min, representing the (a) center and (b) edge regions of the polished cross section

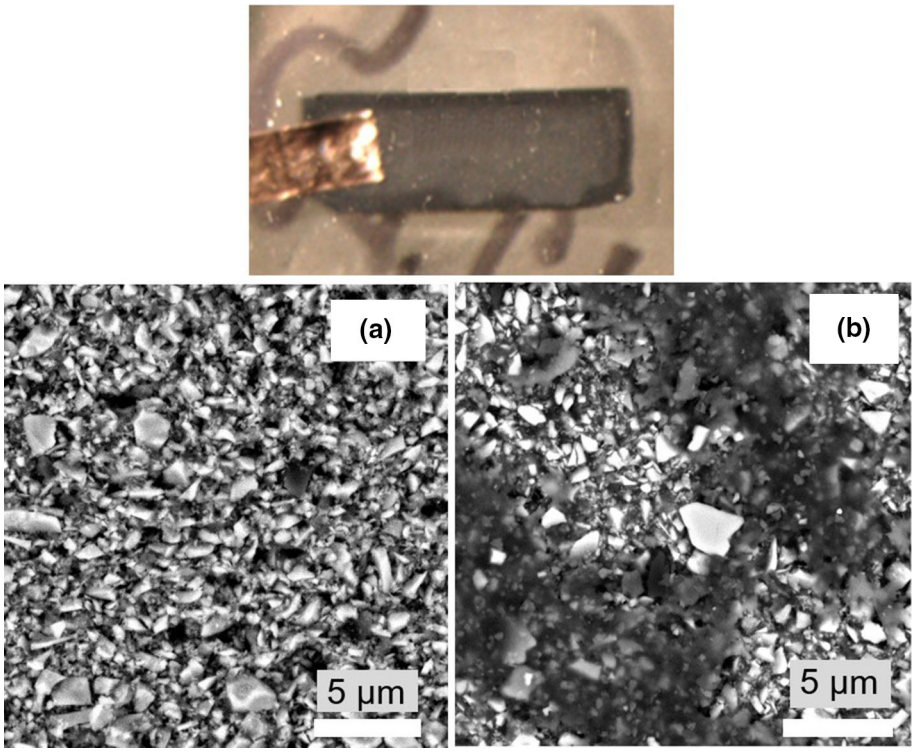

Fig. 7 SEM images of SiC-B_4C-C sintered under 100% *H*-field at 1450 °C and held for 30 min, representing polished cross sections of the (a) center and (b) edge regions

behavior. WC has been heated effectively under magnetic fields, despite the fact that it is non-magnetic. B_4C has shown non-magnetic and non-conducting behavior at relatively low temperatures (below 800 °C). Above this temperature, it has become more electrically conductive, behaving like a metal. From Fig. 2, it can be noted that both SiC and B_4C reach their

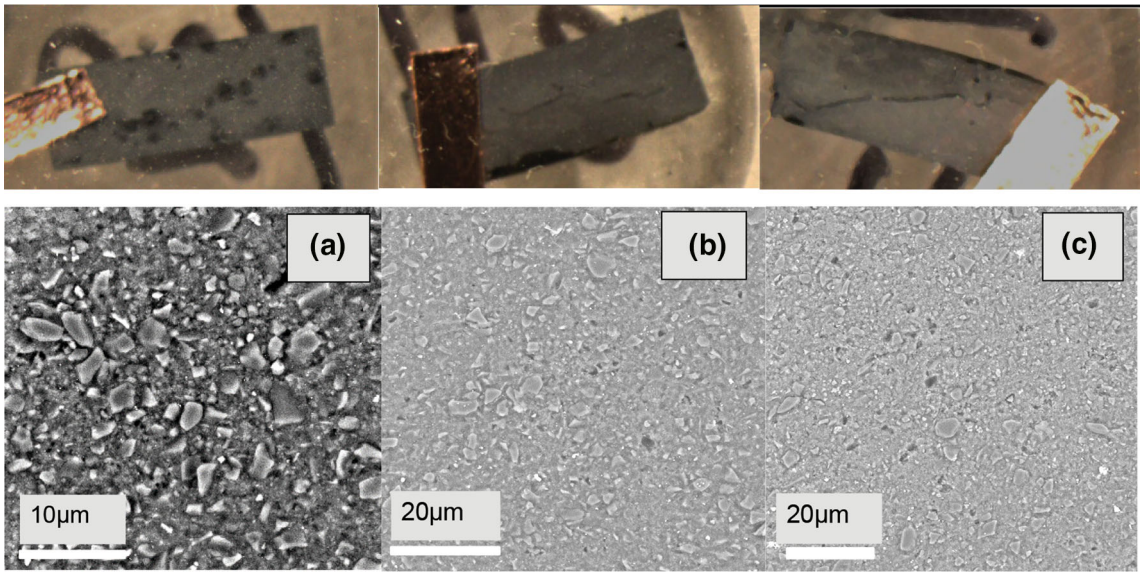

Fig. 8 SEM images of B_4C microwave-sintered under (a) 100% *E*-fields at 1050 °C, (b) 50% *E*/*H*-fields at 1300 °C, and (c) 100% *H*-fields at 1500 °C, and held for 30 min, representing cross-sectional regions

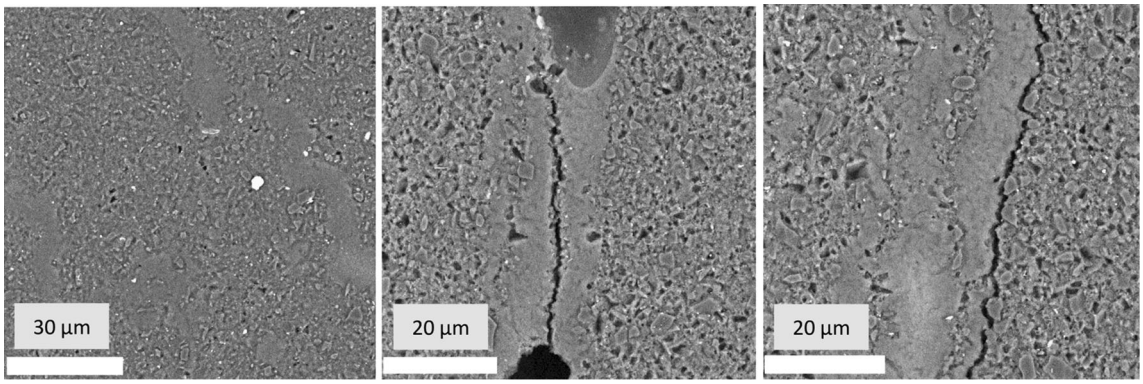

Fig. 9 SEM images of B_4C microwave-sintered under 100% *H*-fields and held at 1500 °C for 30 min, representing polished cross sections and showing fully dense regions. Particles on the surface were identified using EDS, as SiC particles could have originated from the milling media

highest temperatures under 100% *H*-field conditions. Since SiC and B_4C have demonstrated non-magnetic and conductive behavior at elevated temperatures, it has been hypothesized that the losses responsible for increased heating under *H*-fields could be due to the formation of eddy currents caused by the varying magnetic fields.

4. Conclusions

Single-mode microwave sintering experiments of SiC, B_4C, and SiC-B_4C-C samples determined that the highest temperatures were achieved under 100% *H*-field conditions, even though ceramics typically couple better under 100% *E*-fields. At elevated temperatures, SiC and B_4C transitioned from insulating to semi-conducting materials, which was one possible explanation for the increased coupling of these ceramics under magnetic field conditions. Microwave sintering of SiC pellets resulted in fully dense regions near the edges, which may have been due, in part, to the Al_2O_3 porous sample mount acting as a sintering aid. However, the highest temperatures of 1500 °C were not sufficient for fully densifying the materials. Addition of B_4C and C to SiC samples improved sinterability, but a skin effect restricted sintering to the outer edges. In contrast, B_4C densification appeared to be relatively homogeneous throughout the samples. Overall, it was concluded that SMMW temperatures higher than 1500 °C were required to produce fully sintered SiC, B_4C, and SiC-B_4C-C samples. SMMW sintering of SiC-B_4C composites will be further investigated using reaction-bonding techniques due to their potentially lower-temperature requirements. The use of gettered gas flow could also be beneficial for minimizing oxidation at high temperatures. Hybrid heating techniques and optimization of dopant concentrations are also expected to improve densification of SiC and B_4C under microwave fields.

Acknowledgments

The authors sincerely thank Dr. Jerry LaSalvia (CTMB, ARL) for helpful discussions, Dr. Victoria Blair (CTMB, ARL) for help

with initial ball milling of SiC-B_4C-C powders, Dr. Steve Kilczewski (CTMB, ARL) for help with cold isostatic pressing of samples, and Ms. Aubrey Fry (CTMB, ARL) and Ms. Carli Moorehead (CTMB, ARL) for help with powder characterization measurements. S.V. Raju was sponsored by the CCDC Army Research Laboratory (ARL) under Cooperative Agreement No. W911NF-16-2-0050. The views and conclusions contained in this document are those of the authors and should not be interpreted as representing the official policies, either expressed or implied, of ARL or the US Government. The US Government is authorized to reproduce and distribute reprints for government purposes notwithstanding any copyright notation herein. The research reported in this document was performed in connection with contract/instrument W911QX-16-D-0014 with the ARL. The views and conclusions contained in this document are those of SURVICE Engineering and ARL. Citation of manufacturer's or trade names does not constitute an official endorsement or approval of the use thereof. The US Government is authorized to reproduce and distribute reprints for government purposes notwithstanding any copyright notation hereon.

References

1. R. Raj, Joule Heating during Flash-Sintering, *J. Eur. Ceram. Soc.*, 2012, **32**, p 2293-2301
2. E.A. Olevsky, S.M. Rolfing, and A.L. Maximenko, Flash (Ultra-Rapid) Spark-Plasma Sintering of Silicon Carbide, *Sci. Rep.*, 2016, **6**, p 33408
3. K.I. Rybakov, E.A. Olevsky, and E.V. Krikun, Microwave Sintering: Fundamentals and Modeling, *J. Am. Ceram. Soc.*, 2013, **96**(4), p 1003-1020
4. R. Pavlacka, C. Brennan, V. Blair, R. Brennan, C. Fountzoulas, J. Cheng, and D. Agrawal, Single-Mode Microwave Sintering of Er:Al_2O_3, *Process. Prop. Adv. Ceram. Compos. VII: Ceram. Trans.*, 2016, **252**, p 3-11
5. R.R. Mishra and A.K. Sharma, Microwave-Material Interaction Phenomena: Heating Mechanisms, Challenges and Opportunities in Material Processing, *Compos.: Part A*, 2016, **81**, p 78-97
6. M. Madhan and G. Prabhakaran, Microwave Versus Conventional Sintering: Microstructure and Mechanical Properties ofAl_2O_3-SiC Ceramic Composites, *Boletín de la Sociedad Española de Cerámica y Vidrio*, 2019, **58**, p 14-22
7. M. Oghbaei and O. Mirzaee, Microwave Versus Conventional Sintering: A Review of Fundamentals, Advantages and Applications, *J. Alloys Compd.*, 2010, **494**, p 175-189
8. X.-J. Gao, J.-W. Cao, L.-F. Cheng, D.-M. Yan, C. Zhang, and P. Man, Effect of Carbon Content on Mechanical Properties of SiC/B_4C Prepared by Reaction Sintering, *J. Inorg. Mater.*, 2015, **30**, p 102
9. X.-J. Gao, J.-W. Cao, L.-F. Cheng, D.-M. Yan, C. Zhang, P. Man, C. Wang, F. Huang, Y. Jiang, Y. Zhou, L. Du, and G. Mera, A Novel Oxidation Resistant SiC/B_4C/C Nanocomposite Derived from a Carborane-Containing Conjugated Polycarbosilane, *J. Am. Ceram. Soc.*, 2012, **95**, p 71-74
10. X.-J. Gao, L.-F. Cheng, J.-W. Cao, D.-M. Yan, C. Zhang, P. Man, J.-F. Qu, Y.-W. Zhou, and S.-J. Sun, Effect of Carbon Contents on Microstructure of B_4C/SiC Composites, *Optoelectron. Adv. Mater. Rapid Commun.*, 2015, **9**, p 482-487
11. R. Rocha and F. Melo, Pressureless Sintering of B_4C-SiC Composites for Armor Applications, *Ceram. Eng. Sci. Proc.*, 2010, **30**(2010), p 113-119
12. Z. Zhang, X. Du, W. Wang, Z. Fu, and H. Wang, Preparation of B_4C-SiC Composite Ceramics Through Hot Pressing Assisted by Mechanical Alloying, *Int. J. Refract. Met. Hard Mater.*, 2013, **41**, p 270-275
13. C.H. Jung and C.H. Kim, Sintering and Characterization of Al_2O_3-B_4C Composites, *J. Mater. Sci.*, 1991, **26**, p 5037-5040
14. X. Lin and P.D. Ownby, Pressureless Sintering of B_4C Whisker Reinforced Al_2O_3 Matrix Composites, *J. Mater. Sci.*, 2000, **35**, p 411-418
15. G. Gorny, M. Raczka, L. Stobierski, L. Wojnar, and R. Pampuch, Microstructure Property Relationship in B_4C-β-SiC Materials, *Solid State Ion*, 1997, **101**, p 953-958
16. L. Stobierski and A. Gubernat, Sintering of Silicon Carbide II. Effect of Boron, *Ceram. Int.*, 2003, **29**, p 355-361
17. P.T.B. Shaffer, Solubility of Boron in Alpha Silicon Carbide, *Mater. Res. Bull.*, 1970, **5**, p 519-521
18. G. Mugnai, G. Beltrami, and L. Piotti Minoccari, Pressureless Sintering and Properties of Alpha SiC-B_4C Composite, *J. Eur. Ceram. Soc.*, 2001, **21**, p 633-638
19. R. Hamminger, Carbon Inclusions in Sintered Silicon Carbide, *J. Am. Ceram. Soc.*, 1989, **72**, p 1741-1744
20. J.A. Menéndez, A. Arenillas, B. Fidalgo, Y. Fernández, L. Zubizarreta, E.G. Calvo, and J.M. Bermúdez, Microwave Heating Processes Involving Carbon Materials, *Fuel Process. Technol.*, 2010, **91**, p 1-8
21. B. Vos, J. Mosman, Y. Zhang, E. Poels, and A. Bliek, Impregnated Carbon as a Susceptor Material for Low Loss Oxides in Dielectric Heating, *J. Mater. Sci.*, 2003, **38**, p 173-182
22. S. Ahmadbeygi, M. Khodaei, A. Nemati, and O. Yaghobizadeh, Fabrication of SiC Body by Microwave Sintering Process, *J. Mater. Sci.: Mater. Electron.*, 2017, **28**, p 5675-5685
23. C. Singhal, Q. Murtaza, and P. Alam, Microwave Sintering of Advanced Composites Materials: A Review, *Mater. Today Proc.*, 2018, **5**, p 24287-24298
24. V.L. Blair, S.V. Raju, M. Kornecki, and R.E Brennan, Single-Mode Microwave Sintering of Traditionally Resistant Materials, *ARL Tech. Rep.,* 8466 (2017)
25. J. Cheng, R. Roy, and D. Agrawal, Radically Different Effects on Materials by Separated Microwave Electric and Magnetic Fields, *Mater. Res. Innov.*, 2002, **5**, p 170-177
26. J. Cheng, D. Agrawal, S. Komarneni, M. Mathis, and R. Roy, Microwave Processing of WC-Co Composites and Ferroic Titanates, *Mater. Res. Innov.*, 1997, **1**, p 44-52
27. E. Breval, J. Cheng, D. Agrawal, P. Gigl, A. Dennis, R. Roy, and A. Papworth, Comparison Between Microwave and Conventional Sintering of WC/Co Composite, *Mater. Sci. Eng. A- Struct. Mater. Prop. Microstruct. Process.*, 2005, **391**, p 285-295
28. Thuault, S. Marinel, E. Savary, R. Heuguet, S. Saunier, D. Goeuriot, and D. Agrawal, Processing of Reaction-Bonded B_4C-SiC Composites in a Single-Mode Microwave Cavity, *Ceram. Int.*, 2013, **39**, p 1215-1219
29. S. Brunauer, P.H. Emmett, and E. Teller, Adsorption of Gases in Multimolecular Layers, *J. Am. Chem. Soc.*, 1938, **60**, p 309-319
30. K.S.W. Sing, D.H. Everett, R.A.W. Haul, L. Moscou, R.A. Pierotti, J. Rouquerol, and T. Siemieniewska, Reporting Physical Adsorption Data for Gas/Solid Systems with Special Reference to the Determination of Surface Area and Porosity (IUPAC Recommendations 1984), *Pure Appl. Chem.*, 1984, **57**(1985), p 603-619
31. J. Rouquerol, D. Avnir, C.W. Fairbridge, D.H. Everett, J.H. Haynes, N. Pernicone, J.D.F. Ramsay, K.S.W. Sing, and K.K. Unger, Recommendations for the Characterization of Porous Solids (IUPAC Recommendations 1994), *Pure Appl. Chem.*, 1994, **66**(1994), p 1739-1758
32. D. Demirskyi and O. Vasylkiv, Microstructure and Mechanical Properties of Boron Suboxide Ceramics Prepared by Pressureless Microwave Sintering, *Ceram. Int.*, 2016, **42**, p 14282-14286